Presented at the International
Conference on Applications of the
Mössbauer Effect, Galilee, Israel,
August 27-31, 1972

LBL-1210

HIGH-RESOLUTION MÖSSBAUER SPECTROSCOPY WITH TANTALUM-181

G. Kaindl and D. Salomon

August 1972

AEC Contract No. W-7405-eng-48

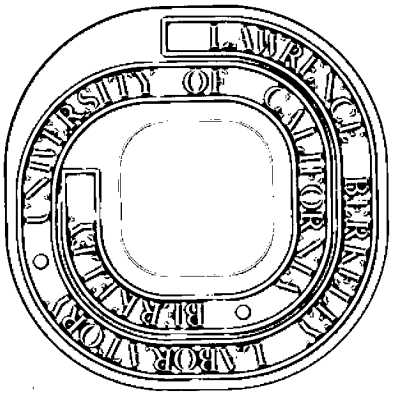

LBL-1210

DISCLAIMER

LBL-1210

HIGH-RESOLUTION MÖSSBAUER SPECTROSCOPY WITH TANTALUM-181

G. Kaindl and D. Salomon

Lawrence Berkeley Laboratory
University of California
Berkeley, California 94720

I. INTRODUCTION

An improvement of the resolution that may be obtained with the Mössbauer method is of considerable interest. The few Mössbauer resonances with lifetimes in the microsecond region have therefore attracted special attention. These are the 93 keV γ transition of ^{67}Zn ($T_{1/2}$ = 9.3 μs), the 6.2 keV γ transition of ^{181}Ta ($T_{1/2}$ = 6.8 μs), and the 13.6 keV γ transition of ^{73}Ge ($T_{1/2}$ = 4.6 μs). Only for the first two cases has the Mössbauer resonance been observed up to now [1,2].

The ultimate resolution which may eventually be reached in a Mössbauer measurement of hyperfine interactions is mainly determined by the natural linewidth of the Mössbauer γ rays and by the size of the pertinent nuclear parameters. For studies of isomer shifts, magnetic dipole, and electric quadrupole interactions, these are the change of the mean-square nuclear charge radius $\Delta \langle r^2 \rangle$, the magnetic dipole moment μ, and the electric quadrupole moment eQ for both nuclear states involved. Since all of them are very large for the 6.2 keV γ resonance of ^{181}Ta [3-5], and comparatively much larger than those known or expected for the γ resonances of ^{67}Zn and ^{73}Ge, the ^{181}Ta resonance may be considered as the top candidate for high-resolution Mössbauer spectroscopy applied to the study of hyperfine interactions.

This high sensitivity, on the other hand, makes the

6.2 keV γ resonance extremely vulnerable to lattice imperfections or impurities, resulting in relatively serious experimental difficulties. That may be the main reason why, until recently, this resonance has not been applied to the study of hyperfine interactions. Most of the work done concentrated on the problem of observing the resonance at all [1,6].

After the initial success of Sauer et al. [4,6], who measured the magnetic splitting of the 6.2 keV γ rays in a longitudinal external magnetic field of only 1.45 kOe, the subject was further studied by two groups, in Munich and in Berkeley. The present paper is based on experimental results obtained by the Berkeley group, but we would like to point out that part of our results, especially the systematics of isomer shifts in transition metals, the electric quadrupole splitting in rhenium metal, and the TaC spectrum, have also been obtained by the Munich group [7].

The paper is divided in three main parts, dealing with magnetic dipole interactions, electric quadrupole interactions, and isomer shift studies. A brief experimental section in the beginning is devoted to the special technique appropriate for the ^{181}Ta γ resonance.

II. EXPERIMENTAL TECHNIQUE

The extreme sensitivity of the 6.2 keV γ resonance to lattice imperfections, as well as the low γ ray energy, and the unusual large ratios of lineshifts to linewidths, require some refinements of the usual Mössbauer technique which will mentioned briefly. Further details are reported elsewhere [17].

A. Source and Absorber Preparation

Two advantageous experimental features of the ^{181}Ta resonance are the almost 100% natural abundance of ^{181}Ta, and the easily preparable source activity of ^{181}W ($T_{1/2}$ = 140 d). For the present experiments it was produced with high specific activity by neutron irradiation of 93% enriched ^{180}W metal in a thermal neutron flux of $3 \cdot 10^{15}$ n/cm^{2}s for periods of at least 30 days. All the sources used were prepared by diffusing the ^{181}W activity into high-purity, and in most cases single-crystal transition metals in high-

vacuum ($\sim 10^{-8}$ Torr) and at temperatures up to 2500°C. Prior to diffusion, the ^{181}W activity, dissolved in concentrated $HF-HNO_3$, was dropped onto the electropolished metal discs and reduced in hydrogen atmosphere (with the exception of the Pd source). Induction heating was used in all cases to heat the metal discs.

The Ta metal absorber used was prepared from a high-purity Ta foil (99.996% pure), rolled to a thickness of 4.1 mg/cm^2, and annealed for 10 h at 2000°C in ultra-high vacuum at $\sim 10^{-9}$ Torr.

One of the difficulties in studying Ta compounds is the necessity of using thin and holefree absorbers due to the large photoabsorption cross-section of Ta for the 6.2 keV γ rays (σ_{ph} = 330 cm^2/g). These were obtained by sedimentating the finely powdered compounds in a benzene-polystyrene solution on 0.25 mil thick mylar foils. Naturally this technique is limited to rather stable compounds.

B. Mössbauer Spectrometer

A conventional sinusoidal velocity spectrometer [8] was used for the Doppler shift measurements. Both the moved source and the fixed absorber were mounted in an evacuated space in order to prevent acoustic disturbances. The 6.2 keV γ rays were detected with an Ar/CH_4-filled proportional counter.

In cases with a large isomer shift/linewidth ratio, the experiments were performed with small solid angles in order to prevent excessive geometrical broadening of the lines, coupled with a corresponding decrease in the observed resonance effect. In these cases as many as 2048 channels were used for recording the spectra.

III. RESULTS AND DISCUSSION

A. Magnetic Splitting

The magnetic splitting of the 6.2 keV γ rays in an external magnetic field was measured with both a velocity drive and a "magnetic drive" [4], using a source of $^{181}W(\underline{W})$

and a Ta metal absorber [11]. The velocity spectra are shown in Fig. 1. The single-line spectrum is quite asymmetric due to the interference effect between photoelectric absorption and nuclear resonance absorption, followed by internal conversion [9,10]. This effect was first observed by Sauer et al. [4]. For the magnetically split spectrum, the source was attached onto the flat surface of a cylindrically shaped Sm-Co permanent magnet, producing a longitudinal magnetic field of 2.93±0.03 kOe at the position of the source.

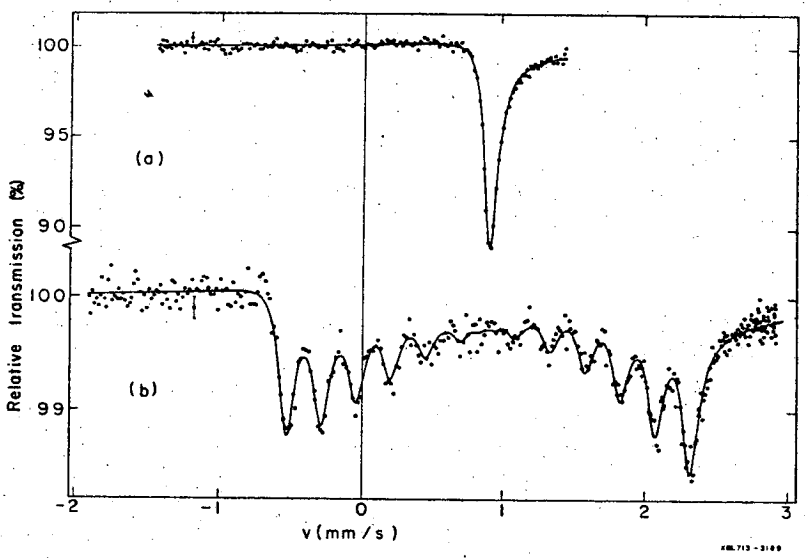

Fig. 1. Velocity spectra of the 6.2 keV γ rays, measured with a $^{181}W(\underline{W})$ source and a single line Ta metal absorber: (a) unsplit source, (b) source in a longitudinal magnetic field of 2.93±0.02 kOe.

The spectra were fitted with dispersion modified Lorentzian lines of the form

$$N(v) = N(\infty) - A(1 - 2\xi X)/(1 + X^2)$$

with $X = 2(v - v_o)/W$. Here $N(v)$ is the intensity transmitted at relative velocity v, v_o is the position of the line, W is the full linewidth at half-maximum, and A is the amplitude of the line. The parameter ξ determines the relative magnitude of the dispersion term. According to Trammel et al. [9] the maximum value for ξ is given by

$$\xi = \left(\frac{\alpha \, \sigma_e'}{6\pi \, \lambda\!\!\!^{-2}} \right)^{1/2}$$

where σ_e' is the partial cross section for E1 photoelectric absorption, α is the internal conversion coefficient, and $\lambda\!\!\!^{-}$ is the wavelength of the incident γ rays, divided by 2π.

The results obtained from the analysis of the different spectra, including those of the magnetic drive spectrum of Ref. 11, are accumulated in Table 1. The best experimental halfwidth obtained (W/2 = 0.057±0.001 mm/s), uncorrected for finite absorber thickness, corresponds to about 17 times the natural linewidth. However, a maximum resonance effect of 11%, uncorrected for background, has been observed, indicating that a considerable amount of the broadening is due to the very thick Ta metal absorber (effective absorber thickness t = 23).

Table 1. Summary of experimental results obtained with a Ta metal absorber and an unsplit and magnetically split $^{181}W(\underline{W})$ source, respectively.

	Velocity spectra		
	unsplit	magnetically split	Magnetic drive spectrum
W/2 (mm/s)	0.056±0.001	0.066±.002	0.069±0.003
2ξ	-0.31±0.01	-0.31±0.01	-0.35±0.07
IS (mm/s)	0.857±0.005	0.854±0.005	---
g(9/2)/g(7/2)	---	1.78±0.02	1.76±0.04

The experimental value for 2ξ may be compared with theory. Using α = 46±8 [12], and σ_e' = $9.8 \cdot 10^4$ b [13], we obtain 2ξ = -0.31, in very good agreement with our experimental value of 2ξ = -0.31±0.01.

The g-factor ratio is given by the weighted average of the two measurements

$$g(9/2)/g(7/2) = 1.77\pm0.02 \quad .$$

With $\mu(7/2) = +2.35\pm0.01$ n.m. [14] we obtain for the magnetic moment of the 6.2 keV state

$$\mu(9/2) = +5.35\pm0.09 \text{ n.m.}$$

This value agrees with our earlier result [11], but is slightly larger than that of Ref. 4.

Recently, we have also observed the magnetic splitting of the 6.2 keV γ rays in the magnetic hyperfine field of ^{181}Ta impurities in Ni metal at room temperature [15]. From the resulting hyperfine spectrum a value for the magnetic field of ^{181}Ta in nickel at room temperature could be deduced: $H_{hf} = -89.6\pm1$ kOe. This represents the first application of the 6.2 keV γ resonance to the study of magnetic hyperfine interactions.

B. Electric Quadrupole Interaction

A high resolution may also be expected for the study of electric quadrupole interactions (EQI) because of the large electric quadrupole moment of the groundstate of ^{181}Ta, $Q(7/2) = +3.9\pm0.4$ b [3], and the large Sternheimer antishielding factor γ_∞ for the Ta ion, $\gamma_\infty \sim -60$ [16]. Initially, we observed the electric quadrupole splitting of the 6.2 keV γ rays with sources of ^{181}W diffused into high-purity single-crystal rhenium metal. By observing the emission spectrum parallel and perpendicular to the [0001]-direction of the single-crystal ^{181}W(Re)-sources, the assignment of individual transitions to the observed lines could be done unambiguously. From the completely resolved spectra, the sign and magnitude of the electric field gradient (EFG) at the ^{181}Ta site in rhenium metal, the ratio of the quadrupole moments of the excited state to that of the groundstate, and the isomer shift of ^{181}Ta(Re) relative to Ta metal could be derived [5]. A similar study, using a source of ^{181}W diffused into rhenium metal foils with preferred orientation has been undertaken by Wortmann [7].

The velocity spectra obtained with our single-crystal sources are presented in Fig. 2. As the 6.2 keV transition has pure E1 character with the spin sequence 9/2 → 7/2, the hyperfine spectrum resulting from an EQI alone consists of 11 hyperfine components, of which 7 are $\Delta m = \pm 1$ transitions, 3 are $\Delta m = 0$ transitions, and 1 is a mixed transition.

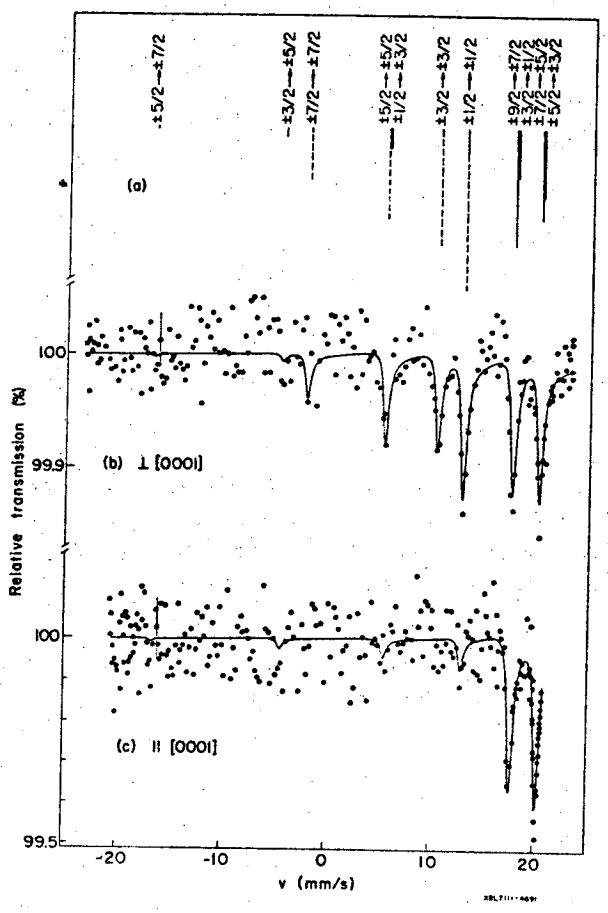

Fig. 2. Velocity spectra of the 6.2 keV γ rays of ^{181}Ta in rhenium metal versus a Ta metal absorber, with direction of observation (b) perpendicular and (c) parallel to the [0001]-axis. In (a) the positions and intensities of the individual components are given, in solid lines for the $\Delta m = \pm 1$ transitions, and in dashed lines for the $\Delta m = 0$ transitions as observed perpendicular to the [0001]-axis.

Both Mössbauer spectra were simultaneously fitted by least-squares with a superposition of dispersion-modified Lorentzian lines, where the amplitude of the dispersion term was set equal to $2\xi = -0.30$. As the only free parameters influencing the line positions, the z-component of the axially symmetric EFG eq, the ratio of the electric quadrupole moments $Q(9/2)/Q(7/2)$, and the isomer shift IS were used.

The results of the least-squares fit analysis are presented in Table 2. For both spectra the total resonance effects, summed over all lines, were only ~ 1%, reflecting the considerable linebroadening observed. Only a small fraction of this (~ 0.1 mm/s for the solid angle $\Omega = 4\pi/500$ used) can be caused by geometrical broadening.

Table 2. Results of analysis of the hyperfine spectra of the single-crystal ^{181}W(Re) sources.

isomer shift (mm/s)	$\frac{Q(9/2)}{Q(7/2)}$	$e^2qQ(7/2)$ (10^{-6} eV)	Linewidth (mm/s)
-14.00±0.10	1.133±0.010	-2.15±0.02	0.60±0.04

With the electric quadrupole moment of the 7/2+ groundstate, $Q(7/2) = +3.9\pm0.4$ b [3], values for the electric quadrupole moment of the 6.2 keV state and for the EFG eq at the ^{181}Ta nucleus in rhenium metal at room temperature can be derived. We obtain

$$Q(9/2) = +4.4\pm0.5 \text{ b}$$

and

$$eq = -(5.5\pm0.5)\cdot10^{17} \text{ V/cm}^2 \quad .$$

The groundstate and the 6.2 keV state of ^{181}Ta have been classified as intrinsic proton states with the Nilsson assignments 7/2+[404] and 9/2-[514], respectively. Neglecting bandmixing, we obtain within the framework of the Nilsson model from our ratio of the spectroscopic quadrupole moments a value for the ratio of the intrinsic quadrupole moments $Q_o(9/2)/Q_o(7/2) = 0.969\pm0.009$, indicating that the

deformation of the 9/2-[514] state may be slightly smaller than that of the 7/2+[404] groundstate.

Using the same experimental technique as for the rhenium experiment, we have additionally measured the hyperfine spectra of the 6.2 keV γ rays of ^{181}Ta impurities in hafnium, osmium and ruthenium metal at room temperature [18]. Some typical velocity spectra are shown in Fig. 3: in (a) for a polycrystalline ^{181}W(Os) source, and in (b) for a single-crystal ^{181}W(Ru) source, with direction of observation perpendicular to the [0001]-direction. The data were analyzed similarly as the rhenium spectra, but in these cases the ratio of the quadrupole moments Q(9/2)/Q(7/2) = 1.133±0.010 was additionally kept constant during the fit procedures.

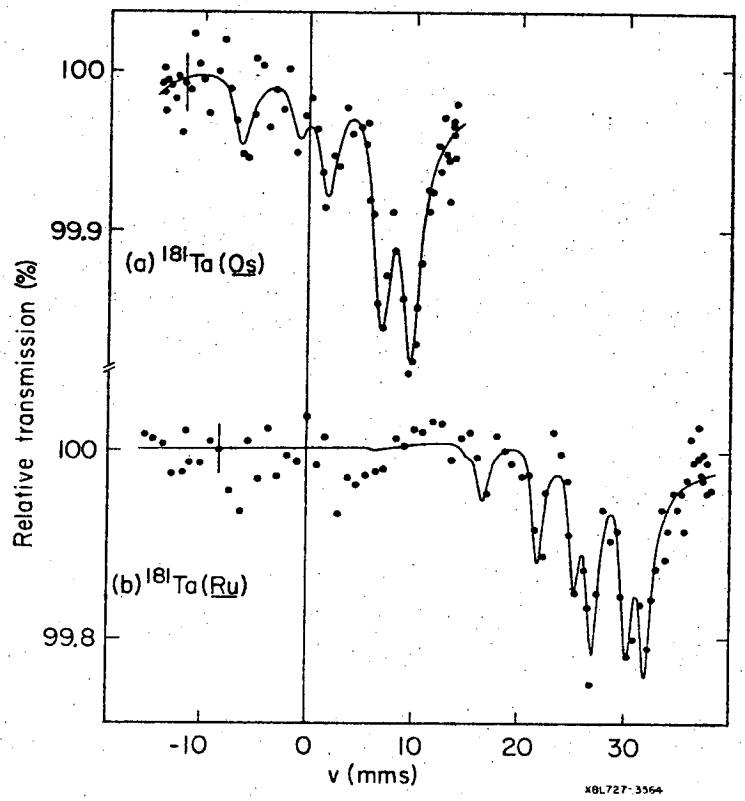

Fig. 3. Mössbauer absorption spectra for sources of ^{181}W(Os) (polycrystalline) (a) and ^{181}W(Ru) (single-crystal, observed perpendicular to the [0001]-axis) (b), both analyzed with a single-line absorber of Ta metal.

The experimental results for the EFGs, including those for rhenium metal, are summarized in Table 3. For all the studied cases the sign of eq was also determined. Our value for the EFG at ^{181}Ta in rhenium metal compares well with the results of nuclear specific heat [19] and nuclear acoustic resonance [20] measurements for pure rhenium metal. Using the quadrupole moment of the groundstate of ^{185}Re ($Q(^{185}Re) = +2.3\pm0.9$ b [21]), a value of $eq = -(4.9\pm1.9)\cdot10^{17}$ V/cm^2 can be derived for the EFG in rhenium metal at 4.2 K. This value is in good agreement with our room temperature result for ^{181}Ta(Re), though of less accuracy due to the large error of $Q(^{185}Re)$.

Table 3. Electric quadrupole interaction of ^{181}Ta impurities in hexagonal transition metals at room temperature.

host	$e^2qQ(7/2)$ (10^{-6} eV)	eq (10^{17} V/cm^2)	W (mm/s)
Re	-2.15±0.02	-5.5±0.5	0.60±0.04
Os	-2.35±0.04	-6.0±0.7	1.8±0.2
Hf	+1.83±0.10	+4.7±0.7	1.6±0.4
Ru	-1.56±0.04	-4.0±0.5	1.3±0.2

Presently, no satisfactory theory exists for EFGs in hexagonal transition metals. Our results show that a simple "point-ion and uniform background model" [22] is not adequate, since the EFGs calculated with its help are positive for all the studied metals, while the experimental values are negative for ^{181}Ta in Re, Os, and Ru metal. Such a model considers only the lattice contribution q_{latt} to the EFG. Obviously, the local contributions, caused by a non-cubic arrangement of localized charge around the central atom as well as by a non-uniform distribution of conduction electrons within the central cell, play an essential role. The latter effect has been considered by Watson *et al.* [23], who predicted an "overshielding effect", caused by the conduction electrons, especially in cases with a high density of states at the Fermi energy. According to this theory, the local conduction electron contributions should be linearly related to the lattice field gradient, $q_{loc} = r\cdot q_{latt}$, so that

we may write for the total EFG

$$q = q_{latt}[(1 - \gamma_\infty) + r(1 - R_Q)] \quad ,$$

where γ_∞ and R_Q are the lattice and atomic Sternheimer factors, respectively. With $\gamma_\infty \sim -60$ [16] and $R_Q \sim -0.2$ [24] for Ta, and using q_{latt} values as calculated with Ref. 22, we may derive overshielding factors r of -160, -85, and -75 for ^{181}Ta in Re, Os, and Ru, respectively. These values are not too different from those predicted for the pure metals, $r \sim -100$ for Re, and $r \sim -55$ for Os [23]. The EFG for ^{181}Ta(Hf), on the other hand, is positive, and even larger that $q_{latt}(1 - \gamma_\infty)$, and its temperature dependence, measured by TDPAC of the 5/2+ state at 482 keV of ^{181}Ta [25], is well described by the anisotropic variation of the lattice parameters with temperature. This means that in this case the lattice contribution may play an essential role.

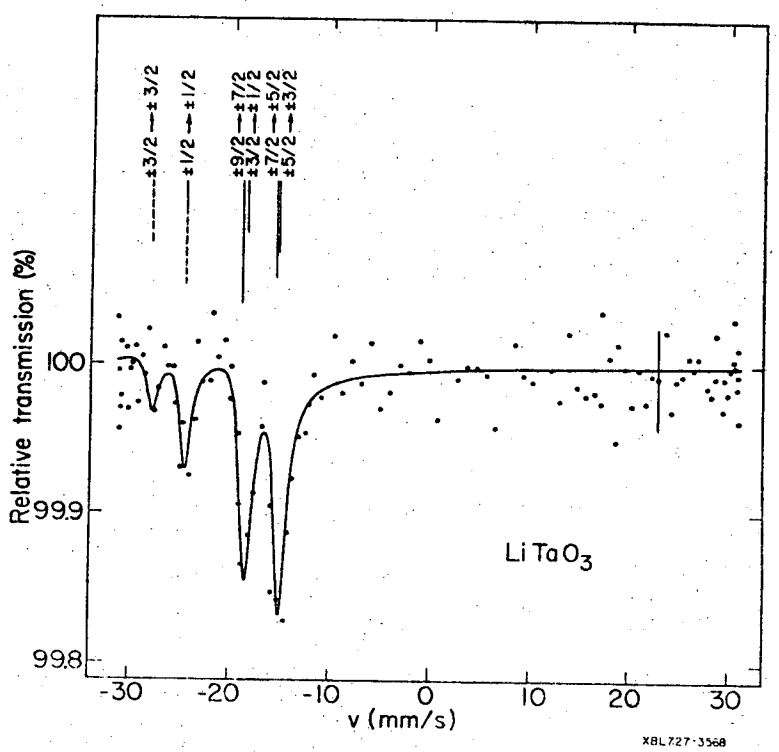

Fig. 4. Hyperfine splitting of the 6.2 keV γ rays in $LiTaO_3$ at room temperature. The position and intensities of the individual components are indicated by solid lines for the $\Delta m = \pm 1$ transitions and by dashed lines for the $\Delta m = 0$ transitions.

We have also applied the 6.2 keV γ resonance to the study of EQI in Ta compounds, namely $LiTaO_3$ and $NaTaO_3$ [26]. At room temperature $LiTaO_3$ is hexagonal, while $NaTaO_3$ is rhombic, with only small deviations from a tetragonal symmetry. The absorbers were prepared from the finely powdered compounds by a sedimentation technique. The resulting hyperfine spectrum for $LiTaO_3$, measured with a $^{181}W(\underline{W})$ source, is shown in Fig. 4. In both cases the absorber preparation technique was found to result in a highly preferred orientation of the axis of the EFG perpendicular to the absorber planes. Therefore, the spectrum shown in Fig. 4 was measured with the absorber plane tilted by 45° to the γ ray direction, in order to get an appreciable intensity in the $\pm 1/2 \rightarrow \pm 1/2$ component, which is necessary for a determination of the sign of the EFG.

Both spectra were fitted under the assumption of an axially symmetric EFG, even though this assumption is exactly valid only for $LiTaO_3$. Both the amplitude of the dispersion term and the ratio of the electric quadrupole moments were kept constant during the fit procedures. The results are given in Table 4, where for completeness also the results for $KTaO_3$ are included.

Table 4. Summary of experimental results for $LiTaO_3$, $NaTaO_3$ and $KTaO_3$. The isomer shift is given relative to a Ta metal absorber.

Compound	IS (mm/s)	$e^2qQ(7/2)$ (10^{-6} eV)	eq (10^{17} V/cm^2)	W/2 (mm/s)
$LiTaO_3$	-24.0±0.3	+2.75±0.06	+7.05±0.80	0.8±0.1
$NaTaO_3$	-13.3±0.3	-1.02±0.07	-2.61±0.45	0.4±0.1
$KTaO_3$	-8.2±0.2	--	--	0.8±0.1

C. Isomer Shifts

The unique features of the 6.2 keV γ resonance among all other Mössbauer transitions are most clearly expressed by the isomer shift results. Until very recently, the only lattices in which the ^{181}Ta γ resonance had been observed,

were W and Ta metal [6]. Then, at about the same time, Wortmann reported on an observation of the resonance for ^{181}Ta(Pt) [27], and the authors published their isomer results for ^{181}Ta impurities in Pt, Ir, Nb, and Mo, and $KTaO_3$ [28].

We have now observed isomer shifts for ^{181}Ta impurities in most of the transition metal hosts, and a few Ta compounds. The isomer shifts cover a total range of 110 mm/s, corresponding to 17,000 times twice the natural linewidth ($W_o = 2\hbar/\tau = 6.436 \cdot 10^{-3}$ mm/s), or 1,600 times the minimum

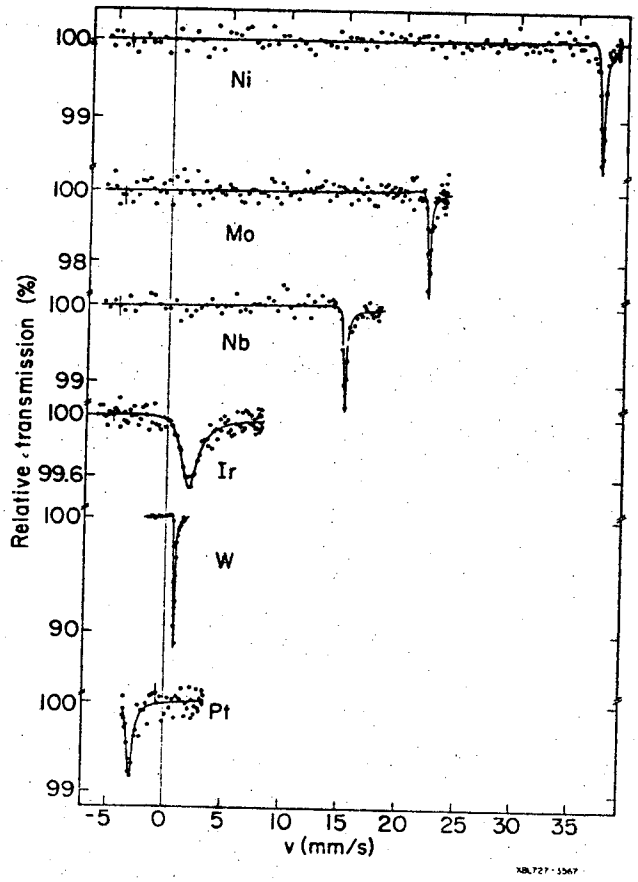

Fig. 5. Single-line spectra for sources of ^{181}W diffused into single-crystal transition metal hosts, analyzed with a Ta metal absorber. The spectrum for the Ni source was measured at 412°C, while all the other spectra were recorded at room temperature.

experimental linewidth obtained up to now [27]. These line-shift to linewidth ratios are more than an order of magnitude bigger than for any other Mössbauer transition presently in use, and the sensitivity of the lineposition of the 6.2 keV γ resonance to subtle solid state effects may therefore be considered as rather unique.

C.1. Systematics of isomer shifts. The isomer shift results reported here were derived from single-line and split spectra. Some representative single-line spectra for metallic sources are shown in Fig. 5. The large range of the isomer shifts is clearly exhibited.

We have also studied isomer shifts for a few compounds, namely $LiTaO_3$, $NaTaO_3$, $KTaO_3$ and TaC [29]. Some typical spectra, all of them recorded with a $^{181}W(\underline{W})$ source, are presented in Fig. 6. So far, the largest isomer shift relative to Ta metal was observed for TaC.

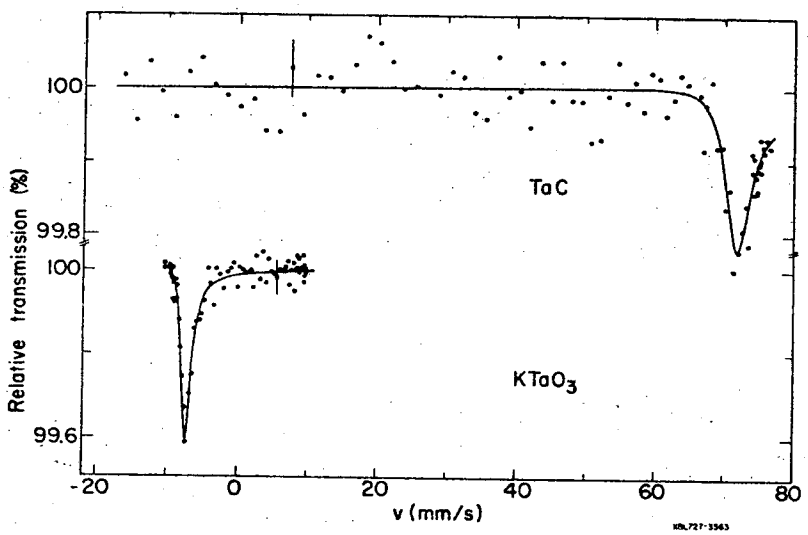

Fig. 6. Single-line absorption spectra for Ta compounds: (a) TaC, and (b) $KTaO_3$.

Table 5 gives a compilation of isomer shift results for both sources and absorbers at room temperature. The value quoted for the Ni lattice was extrapolated from the temperature dependence of the IS, measured for this host metal above the Curie temperature of nickel, taking into account the known temperature dependence of the lattice parameters of nickel.

Table 5. Compilation of isomer shift results, with source and absorber at room temperature. The isomer shifts are given relative to a Ta metal absorber.

Source Lattice	IS (mm/s)	W(FWHM) (mm/s)	Effect (%)
V	-33.6±0.7	7.7±2.6	0.1
Ni	-39.5±0.2	0.50±0.08	1.6
Nb	-15.26±0.10	0.19±0.06	0.5
Mo	-22.50±0.10	0.22±0.03	3.0
Ru	-27.50±0.30	1.3±0.2	0.7
Rh	-28.80±0.25	3.4±0.5	0.3
Pd	-27.55±0.25	2.7±0.6	0.3
Hf	-0.60±0.30	1.6±0.4	0.2
Ta	-0.075±0.004	0.184±0.006	2.4
W	-0.860±0.008	0.112±0.002	11.3
Re	-14.00±0.10	0.60±0.04	1.3
Os	-2.35±0.04	1.8±0.2	0.8
Ir	-1.84±0.04	1.60±0.14	0.5
Pt	+2.66±0.04	0.30±0.08	0.9
Absorbers			
$LiTaO_3$	-24.04±0.30	1.6±0.2	0.9
$NaTaO_3$	-13.26±0.30	1.0±0.2	0.9
$KTaO_3$	-8.11±0.15	1.5±0.2	0.3
TaC	+70.8±0.5	2.4±0.4	0.2

The observed experimental linewidths range from 17 times twice the natural linewidth for the W source up to 1200 times for the V source. The narrowest linewidths are observed for those host metals which are continuously

miscible with Ta metal (with the exception of V). The best lineshift to linewidth ratios are observed for the Mo, Nb and Ni sources, even though the experimental linewidths for these three host metals are up to 77 times the natural one (in the case of nickel). Some of our results, namely the isomer shifts for the host metals V, Mo, Pd, W, Re and Pt, as well as the one for TaC have also been obtained by Wortmann [7,27], and his results are in good agreement with ours.

The isomer shifts for transition metal hosts exhibit some interesting systematic features if plotted versus the number of outer electrons for the series of 3d, 4d and 5d transition metals, as done in Fig. 7. As one can see, they arrange themselves in 3 different groups corresponding to the 3d, 4d and 5d host metals. Without exception, the transition energy decreases when going from a 5d to a 4d and

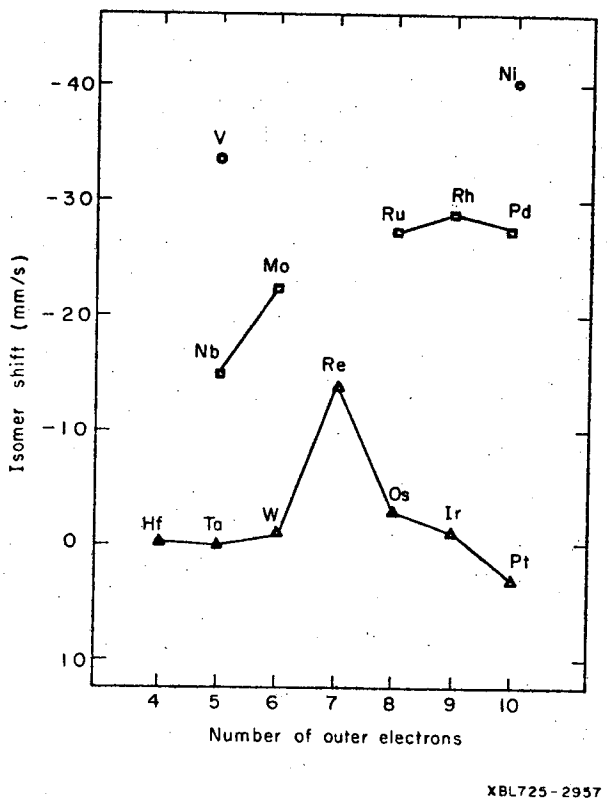

Fig. 7. Systematics of isomer shifts for transition metal hosts.

further to a 3d host element in a vertical column of the periodic system. The same behaviour has previously been observed for the ISs of the 14.4 keV γ rays of ^{57}Fe [30], and more recently by the authors for those of the 77 keV γ rays of ^{197}Au and the 90 keV γ rays of ^{99}Ru [15]. In these cases the changes of the mean square nuclear charge radii are relatively well established [32], at least their signs, so that we may derive from their systematics changes for the total electron density (L) within the nuclear volume. We find that for ^{57}Fe, ^{99}Ru, and ^{197}Au impurities in transition metals the electron density increases when proceeding from a 5d to a 4d and finally to a 3d host metal in a vertical column. The same conclusion can be drawn from less complete isomer shift data of the 73 keV γ rays of ^{193}Ir [33], the 99 keV γ rays of ^{195}Pt [34], and the 36 keV γ rays of ^{189}Os. If we assume the same dependence for the electron density at ^{181}Ta impurities we may conclude that $\Delta\langle r^2\rangle$ is negative for the 6.2 keV γ transition, since the 6.2 keV transition energy decreases when going from 5d to 4d, and finally to 3d host metals in a vertical column of the periodic system (Fig. 7).

From the isomer shifts measured for ^{193}Ir(Ni) and ^{193}Ir(Pt) [33], we derive an electron density difference of $\Delta L(Ir) = L(Ni) - L(Pt) = +3.5\cdot10^{26}$ cm^{-3}, using $\Delta\langle r^2\rangle = 4.6\cdot10^{-3}$ fm^2 [32]. Similarly, we get from our measurements for ^{197}Au(Ni) and ^{197}Au(Pt) [15], using $\Delta\langle r^2\rangle = 1.5\cdot10^{-2}$ fm^2 [35], a value of $\Delta L(Au) = 2.7\cdot10^{26}$ cm^{-3}. If we take the average of the two values and correct for relativistic effects [36], we get $\Delta L(Ta) \sim 2.5\cdot10^{26}$ cm^{-3} between the nickel and platinum hosts. With an isomer shift difference of 42 mm/s between these hosts, we finally deduce

$$\Delta\langle r^2\rangle \sim -1.6\cdot10^{-2} \text{ fm}^2$$

as an estimate for the change of the mean-square nuclear charge radius of the 6.2 keV transition.

This sizable $\Delta\langle r^2\rangle$, combined with the narrow linewidth and the high atomic number of Ta forms the basis for the unique resolution obtainable in isomer shift studies with the 6.2 keV γ rays.

The above arguments, which have been used in a very similar way by Wortmann [7], should only be considered as an order-of-magnitude estimate for $\Delta\langle r^2\rangle$. The absolute value

of $\Delta \langle r^2 \rangle$ may be subject to an appreciable error, but the sign is rather well established. The negative sign for $\Delta \langle r^2 \rangle$ is favoured by the ratio of the intrinsic quadrupole moments $Q_o(9/2)/Q_o(7/2) = 0.969 \pm 0.009$, derived from our experimental ratio of spectroscopic quadrupole moments. Assuming constant volume for the nucleus in both nuclear states, and using a deformation parameter $\beta = 0.275$, we find that the excited state is slightly less deformed than the groundstate by $\Delta\beta = -0.007 \pm 0.0023$; the relation $\Delta \langle r^2 \rangle = 3/2\pi \cdot R_o^2 \, \beta \, \Delta\beta$ leads then to a collective contribution to $\Delta \langle r^2 \rangle$ of $-(4.5^{+1}_{-1.1}) \cdot 10^{-2}$ fm^2.

All our isomer shift results including those for the compounds, are represented graphically in Fig. 8. The bonding in transition metal carbides is not yet well enough understood in order to allow a derivation of $\Delta \langle r^2 \rangle$ from the

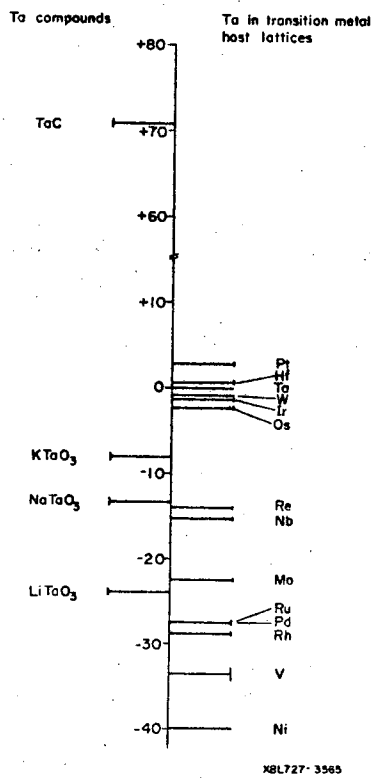

Fig. 8. Graphical representation of isomer shifts for the 6.2 keV γ rays of ^{181}Ta.

measured isomer shift of TaC. Especially, the question of the relative importance of metal-metal and metal-nonmetal bonding is not fully clarified [37-40].

C.2. Temperature dependence of the 6.2 keV gamma ray energy. Probably the best illustration for the high resolution of the 6.2 keV γ resonance is provided by the temperature dependence of linepositions for ^{181}Ta impurities in transition metals. The striking result is that the lineshifts are mainly caused by the temperature dependence of the isomer shift, and not as usually observed (for ^{57}Fe and ^{119}Sn) by the thermal redshift [41,42]. We find that for ^{181}Ta(Ni) the temperature shift of the line position is -33 times the thermal redshift expected for a Debye-solid at high temperature, and amounts to a shift of 2.3 natural widths per degree.

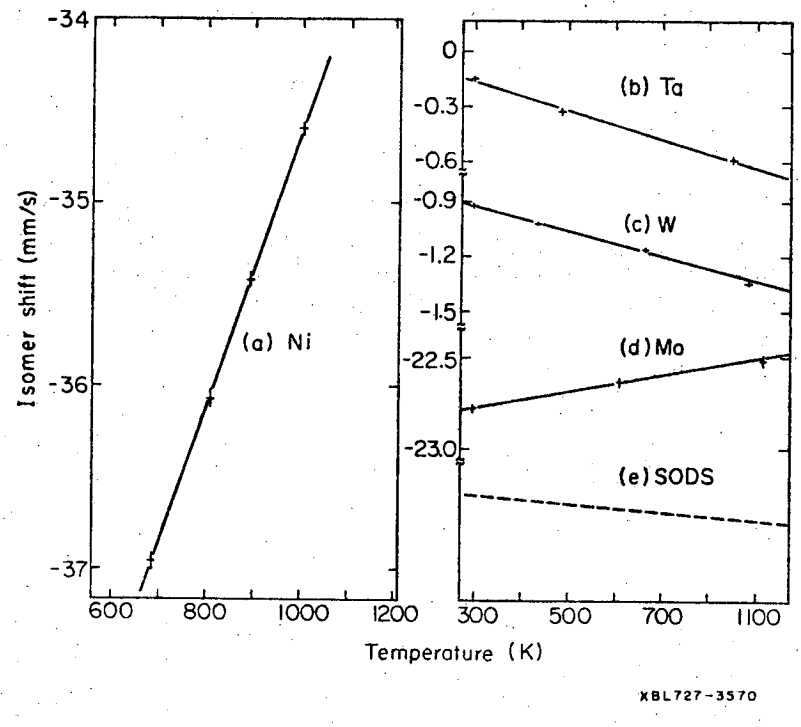

Fig. 9. Temperature dependence of line shifts (relative to a Ta metal absorber at room temperature) for sources of ^{181}W diffused into Ni (a), Ta (b), W (c), and Mo (d). For comparison, the second order Doppler shift expected for a Debye-solid at high temperature is also plotted in (e). All curves are plotted with the same scale on both axis.

The host metals investigated so far are Ta, W, Pt, Mo and Ni. For the experiments the moved sources were heated in a vacuum furnace, the temperature being measured by a Pt-Pt/Rh thermocouple directly in contact with the source metal discs. The fixed Ta metal absorber was kept at room temperature.

Some typical results are shown in Fig. 9. Within the accuracy of our measurements, the data can be described rather well by a linear relationship between lineshift S and temperature. The solid curves are the results of least-squares fits of straight lines to the data.

The influence of the thermal expansion of the lattice on the experimentally observed temperature dependence of the γ ray energy was first discussed by Pound et al. [43]. Combining the temperature shift results for iron metal [41] with the results of high pressure experiments on iron metal [43], they found that only ~ 8% of the temperature shift was caused by the thermal expansion of iron metal. The main part of the experimental shift could very well be described by the second order Doppler shift, assuming a Debye model for iron metal.

More recently, Rothberg et al. [44] have analyzed the temperature shifts of the resonance line for β-tin by additionally taking into account a temperature variation of the electron density at constant volume due to electron-phonon interaction. They find, however, that for β-tin, as in the case of iron metal, the thermal redshift is the dominating cause of the observed temperature shift.

Following Ref. 43 and 44, we may write for the experimentally observed temperature variation of the line-position S

$$\left(\frac{\partial S}{\partial T}\right)_P = \left(\frac{\partial S_{SODS}}{\partial T}\right)_P + \left(\frac{\partial S_{IS}}{\partial T}\right)_V + \left(\frac{\partial S_{IS}}{\partial \ \ln V}\right)_T \left(\frac{\partial \ \ln V}{\partial T}\right)_P$$

The first term represents the second order Doppler shift, which is given for a Debye-solid at high temperatures by $-3k/2Mc$ in cm/s, amounting to $-2.299 \cdot 10^{-4}$ mm/s per degree for the 6.2 keV γ rays of ^{181}Ta. The second term represents the explicit temperature dependence of the isomer shift at

constant volume due to electron density changes caused by the effects of electron-phonon interaction upon the electronic state of the conduction electrons. The third term describes the volume dependence of the isomer shift created by thermal expansion.

The experimental data are summarized in column 2 of Table 6. Our value for $\left(\frac{\partial S}{\partial T}\right)_P$ for the W host lattice agrees quite well with the result of Taylor et al. [45]. From the experimental lineshifts, values for the isobaric temperature dependence of the isomer shift $\left(\frac{\partial S_{IS}}{\partial T}\right)_P$ are derived after applying the correction for thermal redshift. The results are presented in column 3 of Table 6. While for nickel and molybdenum the γ ray energy increases with increasing temperature, the opposite effect is observed for Ta, W and Pt.

Table 6. Isobaric temperature variation of transition energy of the 6.2 keV γ rays, $\left(\frac{\partial S}{\partial T}\right)_P$, for ^{181}Ta impurities in transition metal hosts (column 2). In column 3 the derived fraction due to isomer shift, $\left(\frac{\partial S_{IS}}{\partial T}\right)_P$, is given, and in column 4 the isobaric thermal expansion coefficients extracted from x-ray data for the present temperature region (0-800°C).

host metal	$\left(\frac{\partial S}{\partial T}\right)_P$	$\left(\frac{\partial S_{IS}}{\partial T}\right)_P$	$\left(\frac{\partial \ln V}{\partial T}\right)_P$
	(10^{-4} mm/s deg^{-1})	(10^{-4} mm/s deg^{-1})	(10^{-5} deg^{-1})
Ni	73.2±3.5	75.5±3.5	5.22
Mo	3.6±0.6	5.9±0.5	1.68
Ta	-8.0±0.5	-5.7±0.5	2.03
W	-7.1±0.2	-4.8±0.2	1.42
Pt	-17.6±0.9	-15.3±0.9	2.91

A separation of the isobaric temperature dependence of the isomer shift into an explicitly temperature dependent part and a volume dependent part can presently not be carried out. However, high-pressure isomer shift studies would directly yield the isothermal change with volume $\left(\frac{\partial S_{IS}}{\partial \ln V}\right)_T$, which then could be used to derive values for the explicit temperature coefficients. From the size of the isobaric temperature coefficients we may expect a rather high sensitivity of the transition energy of the 6.2 keV γ rays on hydostatic pressure.

In the case of ^{57}Fe, isomer shifts have been measured for the 14.4 keV γ rays as a function of pressure for ^{57}Fe impurities in a series of 3d, 4d, and 5d transition metal hosts [46]. The isothermal changes with volume were found to be positive in all cases, even though their absolute values showed large variations. The positive sign results from a decrease of the total electron density at the nucleus with increasing volume. Furthermore, the experimental values for $\left(\frac{\partial S_{IS}}{\partial \ln V}\right)_T$, when plotted versus the isomer shifts of the host metals, exhibit a systematic increase with decreasing isomer shift or increasing electron density L, which is not unexpected: a simple scaling of L with the volume, taking into account the opposite contributions of s- and d-like conduction electrons, would result in such a correlation.

A similar behaviour may be expected for the ^{181}Ta case. It would be in agreement with the negative sign for $\Delta \langle r^2 \rangle$ and the observed isobaric temperature shifts. For a qualitative discussion we use a simple scaling assumption [47]

$$\Delta L = - \frac{\Delta V}{V} L_{6s}$$

taking $L_{6s} \sim 2 \cdot 10^{27}$ cm^{-3} for the 6s-density at the Ta nucleus [48]. Then we expect from the thermal expansion of the nickel lattice a value of $\left(\frac{\partial S_{IS}}{\partial \ln V}\right)_T \left(\frac{\partial \ln V}{\partial T}\right)_P \sim 170 \cdot 10^{-4}$ mm/s deg^{-1}, using $\Delta \langle r^2 \rangle = 1.6 \cdot 10^{-2}$ fm^2. This is more than

twice as large as the experimentally observed isobaric variation with temperature. But we have to consider that the simple scaling assumption is probably overestimating the change of electron density with volume [46,47], and that the explicit temperature dependence is expected to be negative for ^{181}Ta. With increasing temperature the electron phonon-interaction should cause a small d → s electron transfer, thus increasing the electron density linearly with temperature [31,44]. Since the observed isobaric temperature variations of the ISs are positive for Ni and Mo, and negative for Ta, W, and Pt, we may expect $\left(\frac{\partial S_{IS}}{\partial T}\right)_V$ to be of a comparable size as $\left(\frac{\partial S_{IS}}{\partial \ln V}\right)_T \left(\frac{\partial \ln V}{\partial T}\right)_P$. If we assume, for an order of magnitude estimate, a transfer of $\sim 10^{-5}$ d-electrons per degree [44], we get $\left(\frac{\partial S_{IS}}{\partial T}\right)_V \sim -21 \cdot 10^{-4}$ mm/s deg^{-1} (using $\Delta \langle r^2 \rangle = -1.6 \cdot 10^{-2}$ fm^2). This effect should depend very critically on the bandstructure.

With this picture the observed temperature variations of the IS can be understood qualitatively: the volume shift is expected to increase with decreasing isomer shift (from 5d to 3d), therefore resulting in positive overall temperature shifts for Ni and Mo. For the 5d elements, the explicit temperature variation is obviously dominant, resulting in small negative overall temperature shifts.

IV. CONCLUSION

The 6.2 keV γ resonance of ^{181}Ta can no longer be considered as an exotic case with limited applications. If experimental problems can be surmounted, its superiour resolution may be of great use for the study of subtle solid-state effects. This was demonstrated especially by the temperature shift results, where the effects caused by hyperfine interaction were found to be dominating over the thermal redshift. One should keep in mind that the present resolution is obtained with experimental linewidths typically of the order of 20 to 100 times the natural linewidth. Even though many applications of its unique features may be achieved with the present linewidths, an improvement is definitely of great interest.

The authors would like to thank Prof. D. A. Shirley for his constant interest in this work and valuable discussions.

REFERENCES

1. W. A. Steyert, R. D. Taylor, and E. K. Storms, Phys. Rev. Letters 14, 739 (1965).
2. H. de Waard and G. J. Perlow, Phys. Rev. Letters 24, 566 (1970).
3. V. S. Shirley, "Table of Nuclear Moments", in Hyperfine Interactions in Excited Nuclei, G. Goldring and R. Kalish, eds., Gordon and Breach, New York (1971) p. 1255.
4. C. Sauer, E. Matthias, and R. L. Mössbauer, Phys. Rev. Letters 21, 961 (1968).
5. G. Kaindl, D. Salomon, and G. Wortmann, Phys. Rev. Letters 28, 952 (1972).
6. C. Sauer, Z. Physik 222, 439 (1969), and references therein.
7. G. Wortmann, Thesis, Technical University Munich (1971).
8. G. Kaindl, Thesis, Technical University Munich (1969).
9. G. T. Trammel and J. P. Hannon, Phys. Rev. 180, 337 (1969).
10. Yu. M. Kagan, A. M. Afanasev, and V. K. Voltovetskii, JETP Letters 9, 91 (1969).
11. G. Kaindl and D. Salomon, Phys. Letters 32B, 364 (1970).
12. A. H. Muir, Jr., Nucl. Phys. 68, 305 (1965).
13. "Table of Mass Absorption Coefficients", Norelco Report, May-June (1962).
14. L. H. Bennett and J. I. Budnick, Phys. Rev. 120, 1812 (1960).
15. G. Kaindl and D. Salomon, this conference.
16. F. D. Feiock and W. R. Johnson, Phys. Rev. 187, 39 (1969).
17. D. Salomon, Thesis, University of California, Berkeley (1972).
18. G. Kaindl and D. Salomon, Phys. Letters 40A, 179 (1972).
19. P. E. Gregers-Hansen, M. Krusius, and G. R. Pickett, Phys. Rev. Letters 27, 38 (1971), and references therein.
20. J. Buttet and P. K. Baily, Phys. Rev. Letters 24, 1220 (1970).
21. J. Kuhl, A. Steudel, and H. Walter, Z. Physik 196, 365 (1966).
22. F. W. DeWette, Phys. Rev. 123, 103 (1961).
23. R. E. Watson, A. C. Gossard, and Y. Yafet, Phys. Rev. 140, A375 (1965).

24. R. Sternheimer, private communication (1972).
25. R. M. Lieder, N. Butler, K. Killig, K. Beck, and E. Bodenstedt, in Hyperfine Interactions in Excited Nuclei, G. Goldring and R. Kalish, eds., Gordon and Breach, New York (1971) p. 449.
26. D. Salomon and G. Kaindl, Bull. Am. Phys. Soc. 17, 681 (1972).
27. W. Wortmann, Phys. Letters 35A, 391 (1971).
28. D. Salomon, G. Kaindl, and D. A. Shirley, Phys. Letters 36A, 457 (1971).
29. The authors are indebted to Dr. N. H. Krikorian, Los Alamos, for the high-purity TaC.
30. S. M. Quaim, Proc. Phys. Soc. (London) 90, 1065 (1967).
31. T. Muto, S. Kobayasi, M. Watanabe, and H. Kozima, J. Phys. Chem. Solids 23, 1303 (1962).
32. G. K. Shenoy and G. M. Kalvius, in Hyperfine Interactions in Excited Nuclei, G. Goldring and R. Kalish, eds., Gordon and Breach, New York (1971) p. 1201.
33. R. L. Mössbauer, M. Lengsfeld, W. von Lieres, W. Potzel, P. Teschner, F. E. Wagner, and G. Kaindl, Z. Naturforschung 26a, 343 (1971); F. E. Wagner, private communication.
34. D. Walcher, Z. Physik 246, 123 (1971).
35. M. Faltens and D. A. Shirley, J. Chem. Phys. 53, 4249 (1970).
36. D. A. Shirley, Rev. Mod. Phys. 36, 339 (1964).
37. L. E. Toth, Transition Metal Carbides and Nitrides, Academic Press, New York (1971).
38. E. Dempsey, Phil. Mag. 8, 285 (1963).
39. R. G. Lye and E. M. Logothetis, Phys. Rev. 147, 622 (1966).
40. V. Ern and A. C. Switendick, Phys. Rev. 137, A1927 (1965).
41. R. V. Pound and G. A. Rebka, Jr., Phys. Rev. Letters 4, 274 (1960).
42. B. D. Josephson, Phys. Rev. Letters 7, 341 (1960).
43. R. V. Pound, G. B. Benedek, and R. Drever, Phys. Rev. Letters 7, 405 (1961).
44. G. M. Rothberg, S. Guimard, and N. Benczer-Koller, Phys. Rev. 1B, 136 (1970).
45. R. D. Taylor and E. K. Storms, Bull. Am. Phys. Soc. 14, 836 (1969).
46. R. Ingalls, H. G. Drickhamer, and G. de Pasquali, Phys. Rev. 155, 165 (1967).
47. L. D. Roberts, D. O. Patterson, J. O. Thomson, and R. P. Levey, Phys. Rev. 179, 656 (1969).
48. Extrapolated from "Relativistic Dirac-Fock Calculations for Os Ions" by J. B. Mann, Los Alamos (1971).

TECHNICAL INFORMATION DIVISION
LAWRENCE BERKELEY LABORATORY
UNIVERSITY OF CALIFORNIA
BERKELEY, CALIFORNIA 94720